

The Scientific Capabilities of the James Webb Space Telescope

Jonathan P. Gardner and the JWST Science Working Group

Jonathan P. Gardner
NASA's GSFC
Code 665
Greenbelt MD 20771
301-286-3938
jonathan.p.gardner@nasa.gov

The Scientific Capabilities of the James Webb Space Telescope

Jonathan P. Gardner and the JWST Science Working Group

1. Introduction

The James Webb Space Telescope (JWST; Figure 1) is a large (25 m^2), cold (<50 K), infrared (IR)-optimized space observatory that will be launched during 2013. It is the successor to the Hubble and Spitzer Space Telescopes. The observatory has four instruments: a near-IR camera, a near-IR multi-object spectrograph, and a tunable filter imager will operate within the wavelength range, $0.6 < \lambda < 5.0 \mu\text{m}$, while the mid-IR instrument will provide both imaging and spectroscopy over the $5.0 < \lambda < 28.5 \mu\text{m}$ spectrum.

During 2008, JWST successfully passed its mission-level Preliminary Design and Non-Advocate Reviews and transitioned to the implementation phase (also known as phase C/D; figure 2). Although the JWST will not be subject to prioritization by the Astro2010 Decadal Survey, it will help to set the scientific context for the future missions that will be reviewed by the Survey. We have also submitted several other white papers that address select aspects of science investigations enabled by the JWST; please see the papers led by Massimo Stiavelli, Rogier Windhorst, George Rieke, Margaret Meixner, George Sonneborn and Mark Clampin.

Further information and detail about JWST has been published in a comprehensive review of JWST science and planned implementation (Gardner et al. 2006, Space Sci. Rev., 123, 485). Information about the current status of JWST is available at: <http://www.jwst.nasa.gov>.

2. Observatory

Image quality: The imaging performance of the telescope will be diffraction limited at $2 \mu\text{m}$, defined as having a Strehl ratio > 0.80 . JWST will achieve this image quality using image-based wavefront sensing and control (WFS&C) of the primary mirror and an attitude control system employing a fine guidance sensor in the telescope focal plane and a fast steering mirror to control observatory induced image motion during observations. The science instrument suite will provide Nyquist sampled imagery at all wavelengths longward of the telescope diffraction limit. The observatory angular resolution is 68 milli-arcsec at $2 \mu\text{m}$. The fine guidance sensor provides a >95% probability of obtaining a guide star for any valid pointing and roll angle combination,



Figure 1. The JWST Observatory. The optical telescope element (OTE) contains the primary and secondary mirrors, the integrated science instrument module (ISIM) element contains the instrumentation and the spacecraft element consists of the spacecraft and the sunshield. Credit: NASA; used with permission.

will be capable of relative pointing offsets with an accuracy of 5 milliarcsec rms, and will be capable of moving-target tracking at linear rates up to 30 milliarcsec s^{-1} above the sidereal rate, sufficient to observe Solar System objects outside the orbit of the Earth.

Table 1. The predicted performance for the JWST Observatory.

Parameter	Capability
Wavelength	0.6 to 28.5 μm
Image quality	Strehl ratio of 0.8 at 2 μm
Telescope FOV	Instruments share \sim 166 arcmin 2 FOV
Orbit	Lissajous orbit about the Sun-Earth L2 point
Celestial sphere coverage	100% annually 39.7% at any given time 100% of sphere has >51 contiguous days visibility Continuous viewing zone <5° from ecliptic pole
Observing efficiency	>70%
Mission life	5 yr design lifetime 10 yr propellant carried for station keeping

Operations: Operations and observing policies for JWST will be similar to those of Hubble, with observing time made available to the international astronomical community through annual peer-reviewed proposals. Each year, the field of regard of JWST sweeps out the whole sky, and every point on the sky is visible for at least 51 contiguous days per year. There are continuous viewing zones within 5 degrees of each ecliptic pole. The observational efficiency, the fraction of the total mission time spent actually “counting photons,” rather than occupied by overhead activities, is expected to be 70%, although this value depends on the specific observing programs that are implemented. The spacecraft will carry enough propellant (the only expendable) to maintain science operations for a 10-year lifetime.

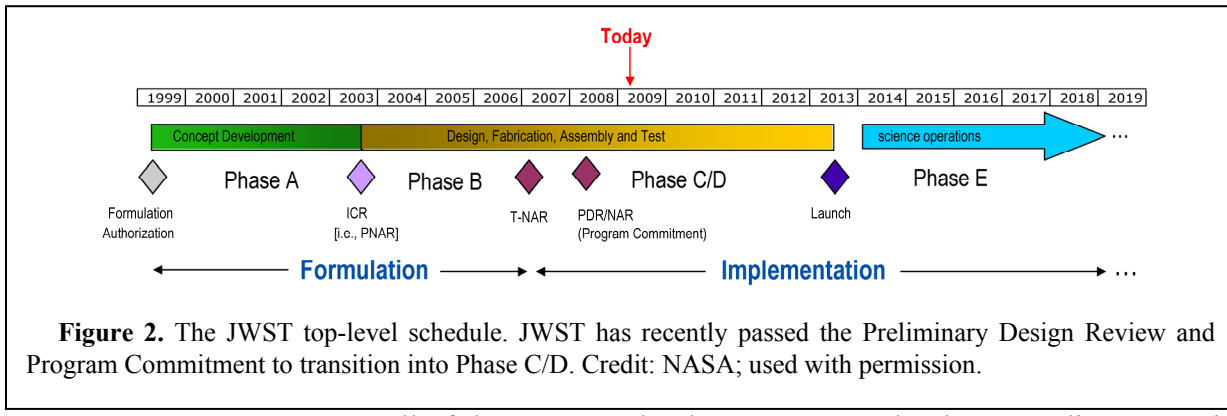


Figure 2. The JWST top-level schedule. JWST has recently passed the Preliminary Design Review and Program Commitment to transition into Phase C/D. Credit: NASA; used with permission.

Current Status: By 2007 all of the JWST technology was at Technology Readiness Level 6, which means demonstrated to work in the relevant space-like environment. The JWST primary mirror consists of 18 beryllium segments of three optical prescriptions. As a consequence, three spare segments are required. Fabrication of all flight and spare segment assembly components is complete, and all segments are currently in the coarse or fine polishing phase. Upon completion of the initial polishing, the segments are built up with the attachment of the mirror actuators onto the back, and cryogenically tested at the X-ray & Cryogenic Facility (XRCF) that was built at

Marshall Space Flight Center to test and calibrate Chandra. Currently, the first flight mirror segment is undergoing thermal vacuum testing in the XRCF. The sunshield is making excellent progress. The flight backplane is being assembled. The mission's Critical Design Review is scheduled for December 2009.

The Integrated Science Instrument Module (ISIM) project's current priority is preparing for its Critical Design Review (CDR) in March 2009. All 4 science instruments plus the guider have been through their own CDRs already. The flight science instruments will be delivered to NASA for integration into the ISIM during 2010. All science instruments flight detectors are in hand.

3. Instrumentation

Table 2 lists the main parameters of the science instruments. Additional information is available at: http://www.stsci.edu/jwst/externaldocs/Instrument_Pamphlets/jwst_pamphlet.pdf.

Table 2. Science instrument characteristics.

Instrument	λ (μm)	Detector	mas/pixel	Field of view
NIRCam Short	0.6 to 2.3	Eight 2048×2048	32	2.2×4.4 arcmin
Long ^a	2.4 to 5.0	Two 2048×2048	65	2.2×4.4 arcmin
NIRSpec MSA ^b	0.6 to 5.0	Two 2048×2048	100	3.4×3.6 arcmin
Slits ^c				~0.2×4 arcsec
IFU				3.0×3.0 arcsec
MIRI Imaging	5.0 to 27.0	1024×1024	110	1.4×1.9 arcmin
Slit ^d	5.0 to 10.0			0.6×5 arcsec
IFU	5.0 to 28.5	Two 1024×1024	200 to 470	3.6×3.6 to 7.5×7.5 arcsec
TFI	1.6 to 4.9 ^e	2048×2048	65	2.2×2.2 arcmin
Guider	0.5 to 5.0	Two 2048×2048	68	2.3×2.3 arcmin

Notes. ^aUse of a dichroic renders the NIRCam long-wavelength FOV cospatial with the short-wavelength channel; the two channels acquire data simultaneously.

^bNIRSpec includes a microshutter assembly (MSA) with four 365×171 microshutter arrays. The individual shutters are each 203 (spectral) \times 463 (spatial) milliarcsec clear aperture on a 267×528 milliarcsec pitch.

^cNIRSpec also includes several fixed slits and an integral field unit (IFU) which provide redundancy and high contrast spectroscopy on individual targets.

^dMIRI includes a fixed slit for low-resolution ($R \sim 100$) spectroscopy over the 5 to $10 \mu\text{m}$ range, and an IFU for $R \sim 3000$ spectroscopy over the full 5 to $28.5 \mu\text{m}$ range. The long wavelength cutoff for MIRI spectroscopy is set by the detector performance, which drops longward of $28.0 \mu\text{m}$.

^eThe TFI wavelength range is 1.6 to $2.6 \mu\text{m}$ and 3.1 to $4.9 \mu\text{m}$, with no sensitivity from 2.6 to $3.1 \mu\text{m}$.

Many JWST observations will be background limited. The background is a combination of zodiacal light, thermal emission from the sunshield and telescope, and stray light. Table 3 lists a subset of instrument sensitivity requirements defined as the point source flux density or emission line flux that yields a 10σ detection in 10,000s of exposure time. Longer or shorter exposures are expected to scale as the square root of the exposure time in background limited cases. It is expected that cosmic-ray hits will limit the maximum integration time for an individual image to

about 1000s, and that longer total exposure times will be achieved through co-adding. Based on experience with Hubble data, for example in the Hubble Deep Field, we expect the errors to scale as the square root of the exposure time in co-adds as long as 10^5 or even 10^6 s. The absolute photometric accuracy requirement is 5% for imaging and 10 to 15% for coronagraphy and spectroscopy, based on calibration observations of standard stars and internal sources.

Table 3. Instrument sensitivities.

Instrument/mode	λ (μm)	Bandwidth	Sensitivity
NIRCam	2.0	R = 4	11.4 nJy, AB = 28.8
NIRCam	3.5	R = 4	13.8 nJy, AB = 28.6
TFI	3.5	R = 100	126 nJy, AB = 26.1
NIRSpec/Low Res.	3.0	R = 100	132 nJy, AB = 26.1
NIRSpec/Med. Res.	2.0	R = 1000	$1.64 \times 10^{-18} \text{ erg s}^{-1} \text{ cm}^{-2}$
MIRI/Broadband	10.0	R = 5	700 nJy, AB = 24.3
MIRI/Broadband	21.0	R = 4.2	$8.7 \mu\text{Jy}, \text{AB} = 21.6$
MIRI/Spect.	9.2	R = 2400	$1.0 \times 10^{-17} \text{ erg s}^{-1} \text{ cm}^{-2}$
MIRI/Spect.	22.5	R = 1200	$5.6 \times 10^{-17} \text{ erg s}^{-1} \text{ cm}^{-2}$

3.1 Near-Infrared Camera (NIRCam)

NIRCam provides multi-filter imaging in the 0.6 to 5.0 μm range. It also includes the ability to sense the wavefront errors of the observatory for alignment of the primary mirror segments. NIRCam's imaging assembly consists of two fully redundant, mirror-image optical trains mounted on two beryllium benches (Figure 3). In each optical train, the incoming light is split by a dichroic into short (0.6 to 2.3 μm) and long (2.4 to 5.0 μm) wavelength light paths. Each beam passes through a filter and pupil wheel, and is onto the detectors with pixel scales of 32 and 65 mas/pixel respectively. The instrument contains a total of ten 2048×2048 detector chips. The short wavelength arm in each optical train contains a 2×2 mosaic of these detectors, while the long wavelength arm contains a single detector covering the same field of view. The detectors arrays are HgCdTe built by Teledyne Imaging Sensors. The filter and pupil wheels contain a range of wide-, medium- and narrow-band filters and WFS&C optics.



Figure 3. The NIRCam engineering test unit optical bench with mass simulators. Credit: NASA; used with permission.

Coronagraphy: NIRCam coronagraphy uses a traditional focal plane coronagraphic mask plate held at a fixed distance from the detectors, so that the coronagraph spots are always in focus at the detector plane. Each coronagraphic plate is transmissive, and contains a series of spots

of different sizes, including linear and radial-sinc occulters, to block the light from a bright object. The coronagraphic plates are selected by rotating into the beam a mild optical wedge in the pupil wheel, which translates the image plane so that the coronagraphic masks are shifted onto the active detector area. Diffraction will also be reduced by apodization at the pupil mask. The pupil wheels will be equipped with a radial sync and line (or bar) occulter with an apodized pupil and integral wedge in each case. Current models predict a contrast of $\sim 10^4$ at 0.5 arcsec, at a wavelength of 4.6 μm .

3.2 Near-Infrared Spectrograph

NIRSpec (Figure 4) is a near infrared multi-object dispersive spectrograph capable of simultaneously observing more than 100 sources over a field-of-view (FOV) of $\sim 3 \times 3$ arcmin. In addition to the multi-object capability, it includes fixed slits and an integral field unit for imaging spectroscopy. Six gratings will yield resolving powers of $R \sim 1000$ and ~ 2700 in three spectral bands, spanning the range 1.0 to 5.0 μm . A single prism will yield $R \sim 100$ over 0.6 to 5.0 μm . Figure 5 shows a layout of the instrument.

Targets in the FOV are normally selected by opening groups of shutters in a micro-shutter assembly to form multiple apertures. The micro-shutter assembly itself consists of a mosaic of 4 subunits yielding an array of 730 (spectral) by 342 (spatial) individually addressable shutters with 203×463 milliarcsec openings and 267×528 milliarcsec pitch. The shutters are opened by sweeping a magnet across the surface of the device, then individual shutters are addressed and released electronically.

The NIRSpec also includes five fixed slits that can be used for high-contrast spectroscopy and a 3 by 3 arcsec entrance aperture for an integral field unit (IFU). The IFU has 30 slices, each 100 milliarcsec wide. Any of the aperture selection devices (micro-shutter assembly, fixed slits or IFU) can be used with any grating choice. The focal plane array is a mosaic of two detectors, each $2k \times 2k$, forming an array of $2k \times 4k$ 100 milliarcsec pixels. The detectors are HgCdTe arrays built by Teledyne Imaging Sensors.

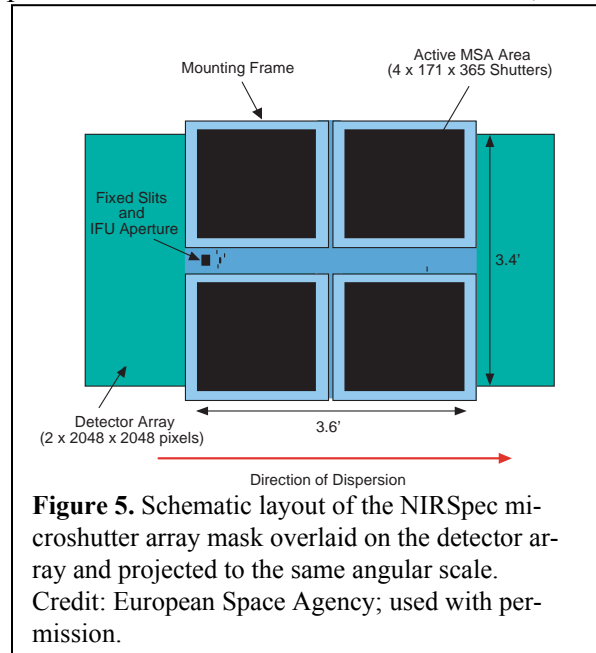


Figure 5. Schematic layout of the NIRSpec microshutter array mask overlaid on the detector array and projected to the same angular scale.
Credit: European Space Agency; used with permission.

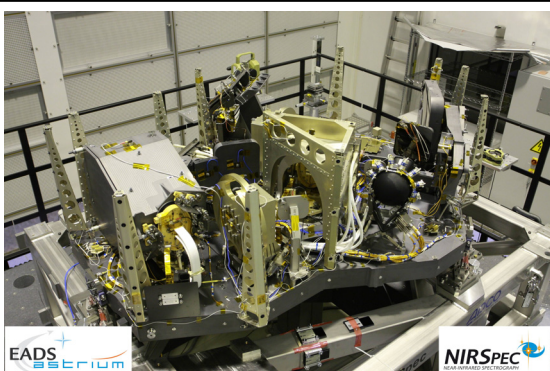


Figure 4. Prototype of the NIRSpec instrument.
Credit: European Space Agency and EADS Astrium; used with permission.

3.3 Mid-Infrared Instrument

The Mid-Infrared Instrument (MIRI; Figure 6) on JWST provides imaging and spectroscopic measurements over the wavelength range 5 to 28.5 μm . The MIRI imager module provides broad-band imaging, and coronagraphy over the above wavelength range, and R~100 slit spectroscopy over 5 – 11 μm using a single 1024×1024 pixel Raytheon Si:As detector with 25 μm pixels. Three quarters of the detector is available for imaging, while the remaining quarter is devoted to the coronagraphic masks and the low-resolution spectrometer. The coronagraphic masks include three phase masks for a quadrant-phase coronagraph and one opaque spot for a Lyot coronagraph. Each quadrant-phase coronagraphic mask has a square field of view of 24×24 arcsec and is optimized for a particular wavelength. The Lyot coronagraph has a field of view of 24×24 arcsec. The imager includes a filter wheel with 12 filters for imaging, 4 filter and diaphragm combinations for coronagraphy, 1 ZnS-Ge double prism for the low-resolution spectroscopic mode, and 1 dark position. The imager has a pixel scale of 0.11 arcsec/pixel and a total field of view of 113×113 arcsec; however, the field of view of its clear aperture is 84×113 arcsec because the coronagraph masks and the low-resolution spectrograph are fixed on one side of the focal plane.

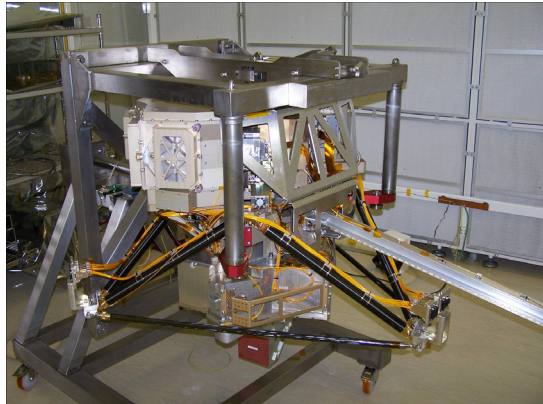


Figure 6. MIRI verification model going into thermal vacuum testing. Credit: European MIRI consortium; used with permission.

mid-infrared bandpasses. Three quadrant phase masks provide high contrast imaging to an inner working angle of λ/D , with band pass of $\lambda/20$, centered at 10.65 μm , 11.4 μm , and 15.5 μm respectively. A fourth, traditional Lyot mask of radius 0.9 arcsec, will provide R ~ 5 imaging at a central wavelength of 23 μm . Simulations predict that the quadrant phase masks will achieve a contrast of $\sim 10^4$ at $3 \lambda/D$. The Lyot stop is predicted to deliver a contrast of 2×10^3 at $3 \lambda/D$.

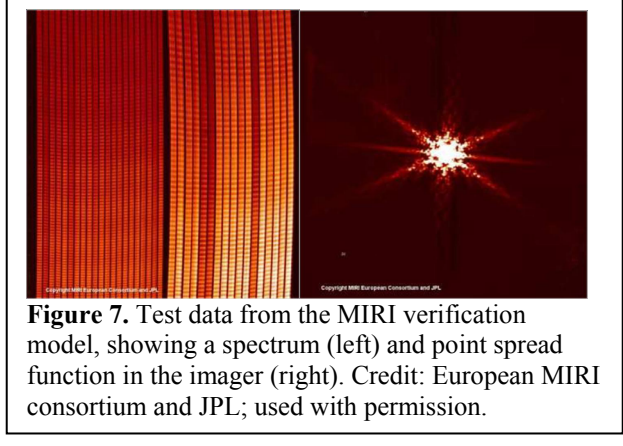


Figure 7. Test data from the MIRI verification model, showing a spectrum (left) and point spread function in the imager (right). Credit: European MIRI consortium and JPL; used with permission.

The integral-field spectrograph (Figure 7) obtains simultaneous spectral and spatial data on a 3×3 to 7×7 arcsec region of sky, depending on wavelength. The light is divided into four spectral ranges by dichroics, and two of these ranges are imaged onto each of two 1024×1024 detector arrays. A full R ~ 3000 spectrum is obtained by taking exposures at each of three settings of the grating wheel.

MIRI features a coronagraph designed for high contrast imaging in selected wavelength-specific

masks provide high contrast imaging to an inner

working angle of λ/D , with band pass of $\lambda/20$,

centered at 10.65 μm , 11.4 μm , and 15.5 μm

respectively. A fourth, traditional Lyot mask of

radius 0.9 arcsec, will provide R ~ 5 imaging

at a central wavelength of 23 μm . Simulations

predict that the quadrant phase masks will

achieve a contrast of $\sim 10^4$ at $3 \lambda/D$. The

Lyot stop is predicted to deliver a contrast of

2×10^3 at $3 \lambda/D$.

3.4 Tunable Filter Imager

The tunable filter imager (TFI; Figure 8) provides Fabry-Perot near-infrared imaging over a field of view of 2.2×2.2 arcmin 2 with a spectral resolution $R \sim 100$. The etalon design allows observations at wavelengths of $1.6 \mu\text{m}$ to $2.6 \mu\text{m}$ and $3.1 \mu\text{m}$ to $4.9 \mu\text{m}$. The gap in wavelength coverage allows a single etalon to reach more than one octave in wavelength.

The TFI uses dielectric-coated etalon plates yielding a finesse of approximately 30. The finesse was chosen to be a compromise between the surface figure requirements and the need to minimize the number of blocking filters, while providing a contrast ratio of about 100. The etalon is scanned using piezo-electric actuators, consisting of lead-zirconia-titanite ceramic transducers.

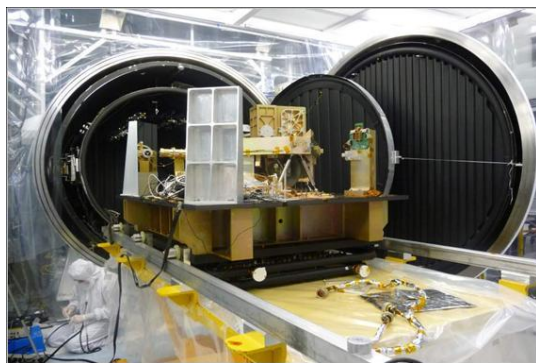


Figure 8. FGS/TFI engineering model in a thermal vacuum chamber. Credit: Canadian Space Agency; used with permission.

The TFI incorporates four hard-edged circular coronagraphic occulting spots (diameter : $0.58''$, $0.75''$, $1.5''$ and $2.0''$) on one side of the field of view, and occupying a region 20 by 80 arcsec. A set of selectable apodization masks is located in the pupil wheel. The coronagraph will deliver a contrast ratio of $\sim 10^{-4}$ (5σ) at 1 arcsec separation. The sensitivity is limited by speckle noise. Contrast ratios of 10^{-5} to 10^{-6} should be achievable beyond 1 arcsec using roll and/or spectral deconvolution techniques. In addition to the coronagraph, TFI features a non-redundant mask (NRM) optimized for point source detection with expected contrast of 10^{-4} to 10^{-5} between 0.1 and 0.5 arcsec. The NRM is optimized to operate between 3.8 and $4.9 \mu\text{m}$.

4. Summary

As the successor to the Hubble and Spitzer Space Telescopes, JWST will be the premier facility-class space telescope in the coming decade. With more than 6 times the collecting area of Hubble, and almost 50 times the collecting area of Spitzer, JWST will open a wide discovery space. Its capabilities will be a key part of the foundation upon which astronomers will build in the coming decade. Operated like Hubble through annual peer-reviewed proposals, it will supply the astronomical community with data and funding to address almost every area of astronomy. JWST discoveries will be released to the news media through press releases, and images will be available to the public through the popular hubblesite.org and the new webbtelescope.org websites.